

# Characterization of a Coherent Optical RF Channelizer Based on a Diffraction Grating

Wenshen Wang, *Member, IEEE*, Richard L. Davis, *Member, IEEE*, Thomas J. Jung, *Student Member, IEEE*, Robert Lodenkamper, *Member, IEEE*, Lawrence J. Lembo, *Member, IEEE*, John C. Brock, *Member, IEEE*, and Ming C. Wu, *Senior Member, IEEE*

**Abstract**—A coherent optical RF channelizer has been constructed and characterized. The optical channelizer is based on a free-space optical diffraction grating, and utilizes coherent optical heterodyne detection to translate all of the frequency channels to a common intermediate frequency (IF). The designed optical channelizer has a 1-GHz channel spacing, and a nominal 5-GHz IF, and can offer an instantaneous bandwidth greater than 100 GHz. The channelizing receiver has been characterized for its frequency response, crosstalk, and spur-free dynamic range, and the results are in a good agreement with the theoretical values.

**Index Terms**—Gratings, optical data processing, optical mixing, optical receiver, optical signal processing, RF photonics.

## I. INTRODUCTION

**F**UTURE military RF systems are increasingly being driven toward higher frequencies and larger bandwidths by user requirements. For example, available communications bandwidth is disappearing as the number of users and the bandwidth per user escalate. This is forcing communications links to ever higher carrier frequencies. Other requirements such as the need for low probability-of-intercept (POI) links are extending the frequencies of planned communications systems out to 60 GHz and beyond. Likewise, modern missile seekers and imaging radars are also moving to frequencies approaching 100 GHz to achieve antenna directivity and higher resolution from small-aperture systems. Realistic considerations of conventional hardware size and power consumption preclude real-time high-resolution monitoring of the entire spectrum; thus, in order to monitor the entire frequency range, the typical electronic warfare (EW) receiver must rapidly step through the entire frequency range in increments of the receiver's instantaneous bandwidth. Currently, the most advanced receivers for processing this signal environment utilize digital electronics and their bandwidths are restricted by the state-of-the-art for electronic analog-to-digital converters to about 1 GHz. Therefore, it is essential to provide a means to coherently channelize the extremely wide-band signal spectrum

into frequency channels with bandwidths that are compatible with digital electronics and with channel outputs that are all translated to a common intermediate frequency (IF).

It is anticipated that many next-generation RF systems will elect to employ optical carrier transmission of RF signals, which will circumvent the very high transmission losses and the sheer bulk attendant with conventional RF cabling and waveguides. Photonic RF signal transmission is already relatively well developed. Recent developments in optical modulators and detectors rapidly are approaching 100-GHz bandwidths with the requisite low noise and distortion. If we can assume that the RF signal is impressed on an optical carrier, it certainly then makes sense to exploit the analog functionality offered by optics to ease the processing load on the electronics. Thus, development is timely for analog processing of wide-band signals in the optical regime.

A photonic channelizer that can process RF signals in parallel will significantly simplify the EW receiver's hardware. Photonic channelization offers many advantages in dealing with ultra-wide-bandwidth RF signals compared to pure electronic solutions. First, it can take the advantage of large instantaneous bandwidth offered by photonics technology that current electronics technology cannot compete with. Second, channelization of broad-band signals and translation into a common IF can greatly reduce the requirement and cost of post-processing electronics. Various embodiments of optical processor architectures have been proposed and demonstrated [1]–[8]. Acoustooptic (AO) systems have been built that are either incoherent [1], producing a power spectrum of the input signal, or coherent [2], [3], in which the output preserves both the amplitude and phase of the input signal. Generally, AO systems are limited in bandwidth to a few gigahertz [4] and, thus, are not suitable for the extremely wide-band applications. Optical techniques for channelizing and frequency-translating wide-band RF signals have been proposed [5] and etalon-based, as well as grating-based channelizers have been built [6], [7]. Additionally wide-band optical channelization can be realized using passive guided-wave optic dispersive components, such as arrayed waveguide gratings (AWGs) [8], fiber Bragg gratings, or fiber Fabry–Perots. To date, these wide-band approaches have not been characterized for their RF performance and none have demonstrated the capability to translate the frequency of the channelized signals to a suitable IF.

In this paper, we report on the construction and performance a coherent photonic RF channelizer that is based on a free-space diffraction grating and utilizes coherent optical heterodyne detection to translate the frequency channels to a predetermined

Manuscript received January 19, 2001; revised May 25, 2001. This work was supported by the Defense Advanced Research Projects Agency through the Air Force Rome Laboratory under Contract F30602-96-C-0026.

W. Wang is with New Focus Inc., Santa Clara, CA 95051 USA.

R. L. Davis, T. J. Jung, and L. J. Lembo are with TRW Inc., Redondo Beach, CA 90278 USA.

R. Lodenkamper is with Informed Diagnostics, Sunnyvale, CA 94085 USA.

J. C. Brock is with Velocium, Redondo Beach, CA 90278 USA.

M. C. Wu is with the Electrical Engineering Department, University of California at Los Angeles, Los Angeles, CA 90095 USA.

Publisher Item Identifier S 0018-9480(01)08703-8.

IF. Such a channelizer can achieve an instantaneous bandwidth of over 100 GHz, with a channel spacing of 1 GHz, and a designed IF of about 5 GHz. In this study, we measured the channel frequency response, crosstalk, and two-tone spur-free dynamic range (SFDR) for our grating-based channelizer. We compared our results to theoretical predictions based on a comprehensive model and found them to be in good agreement.

## II. PRINCIPLE OF THE COHERENT OPTICAL RF CHANNELIZER

In the photonic channelizer, the input lightwave carrying wide-band microwave signals is collimated and made incident on the diffraction grating. The signal's frequency components are dispersed through a range of angles and subsequently imaged onto the detector array. The center position of a detector corresponds to a particular RF frequency and the detector's center-to-center spacing determines the channel spacing. A second beam, i.e., the local-oscillator (LO) beam, is derived from a mode-locked laser whose spectrum comprises an optical frequency comb with a frequency spacing equal to the channel spacing. This beam is made incident on the grating at some offset angle with respect to the signal beam, thereby causing its spectrum to be displaced in the detector plane. Such spatial offset will result in a constant frequency difference between the spatially overlapping signal beam and the LO comb lines at the output plane. This constant frequency shift for every channel is predetermined as the IF. When the two beams are combined on the detectors, each detector generates a heterodyne beat tone. In this way, each photodetector translates a portion of the signal spectrum to the same IF band so that each detector channel may use the same postdetection electronics. A high degree of coherence between the signal beam and the LO comb is required to minimize the phase noise associated with the heterodyne RF signal. Continuous-wave (CW) injection locking of mode-locked lasers has been shown to establish phase coherence between the optical carrier of the signal and the optical frequency comb [9], [10], and we have previously characterized the RF performance of injection locking for this application [11]. The coherent optical channelizer concept is illustrated in Fig. 1.

Key enabling technologies for the photonic RF channelizer are a highly dispersive grating used in conjunction with a low-distortion optical collimating system, the generation of an LO optical frequency comb that can be phase locked to the incoming signal optical carrier, broad-band electrooptic (EO) modulators, and a focal-plane photodetector array. The dispersive element, being the principle component of the optical channelizer, determines the possible system resolution performance and dictates the optical component requirements for the channelizer.

## III. OPTICAL CHANNELIZER TESTBED

We designed and constructed a photonic channelizer testbed to evaluate the merit of this approach for processing extremely wide-band RF signals. Our design used a commercial off-the-shelf diffraction grating and a custom-designed lens assembly that served both to collimate optical-fiber inputs to the grating and to focus the diffracted beams back to the output plane. The grating has a line density of 452 lines/mm, and was used in the

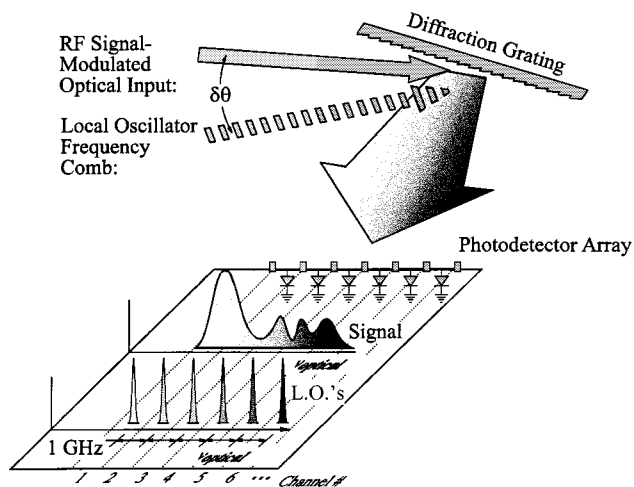


Fig. 1. Coherent optical channelizing receiver that uses a dispersion grating to map the optically carried RF signal and LO spectra onto a photodetector array.

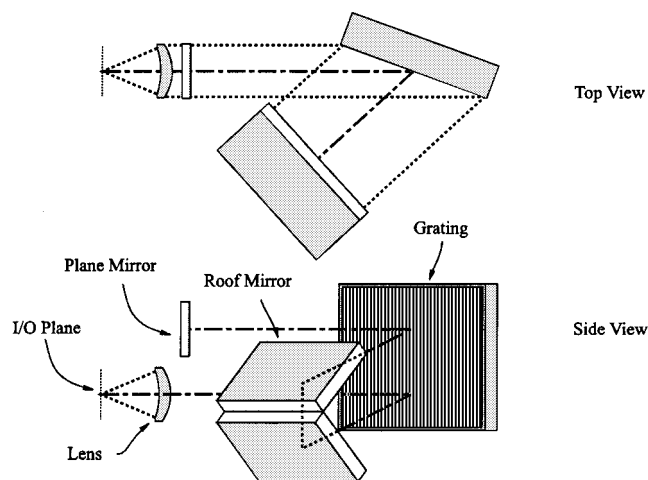


Fig. 2. Channelizer optical layout that uses a single diffraction grating with a multipath optical arrangement.

second order. Our design called for a single grating that was used four times, as shown schematically in Fig. 2. This multipath geometry allowed us to achieve the high optical frequency resolution required for operation of the RF channelizer.

In our basic setup, the input light beams from cleaved single-mode fibers were directed to the lens assembly. The lens design was computer optimized and the design incorporated a beamsplitter. This provided us the flexibility to position the optical and mechanical components for the optical inputs and outputs in two equivalent focal planes, thus simplifying the organization and mounting fixtures for these components. This freedom in laying out the input and output configurations does introduce additional insertion loss that will influence the RF performance of the channelizer. The actual layout of the channelizer input/output optics is illustrated in Fig. 3, which is a scale drawing of the lens showing the beamsplitter and the basic arrangements of the optics used for our RF measurements. A small turning prism was used for the LO input beam, as shown in Fig. 3, to allow for collection of the output beam. Both beams had a vertical and horizontal offset from the optical axis to avoid spatially overlapping the input and output spots

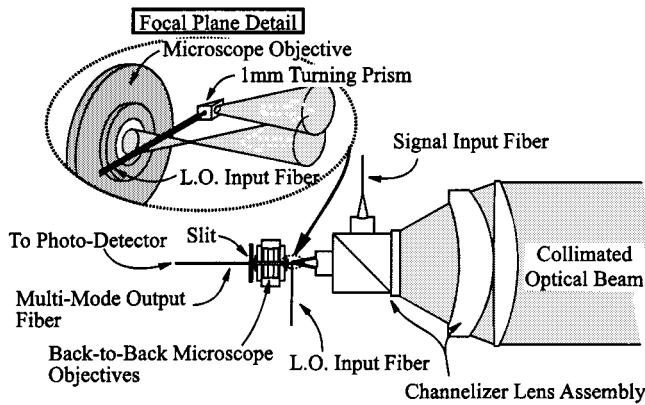


Fig. 3. I/O optical layout for channelizer testbed.

on the focal plane. The displacements from the optical axis, however, were small enough so that the beams are still well within the lens's field-of-view limit. The spatial dispersion in the output plane of the optical channelizer was measured to be  $20 \mu\text{m}/\text{GHz}$ , which was in agreement with the design value. A pair of microscope objectives was used to image the output onto a  $25\text{-}\mu\text{m}$ -wide precision air slit that is placed just in front of a step-index multimode fiber, which is coupled to a 25-GHz photoreceiver. The arrangement of the slit in front of the  $50\text{-}\mu\text{m}$  core fiber served to simulate a single output channel of the photonic channelizing receiver. Repositioning the lenses and slit/output fiber can alter the magnification of the pair of objectives quite simply. This allowed us to control the RF channel bandwidth as desired. We examined the fundamental interdependencies of the RF performance characteristics on the optical layout, e.g., detector pitch, detector fill factor, and focused optical spot sizes and shapes, and these results dictated the detailed optical layout [12]. One noteworthy result of our design analysis was that in order to meet our RF performance goals, the focused LO spot diameter at the output focal plane must be set equal to about one-half of the channel spacing, and the focused signal spot diameter was required to be 3–4 times larger than the LO spot.

We characterized the optical channelizer lens assembly by using a dynamic knife-edge technique. For these measurements, a  $\lambda/20$  flat mirror was placed perpendicular to the optical axis at the output aperture of the lens assembly so that the input fiber beam spot was imaged on the focal plane.

The spot size as measured at the output plane was about  $16 \mu\text{m}$ . We then made a direct measurement of the fiber output and got a value of  $15.5 \mu\text{m}$  at the  $1/e^2$  diameter. This measurement indicated that the lens performance was nearly diffraction limited.

We measured the optical throughput for the signal and LO beam paths through the channelizer. The total insertion loss for the signal beam path was 28 dB and, for the LO path, the total loss was 18 dB. The primary difference in the insertion loss was due to the fact that the signal and LO beams were coupled in from different sides of the input beamsplitter, which was intentionally designed with an asymmetric split ratio in order to maximize the amplitude of the heterodyne beat signal produced by the combination of the transmitted signal and LO beams.

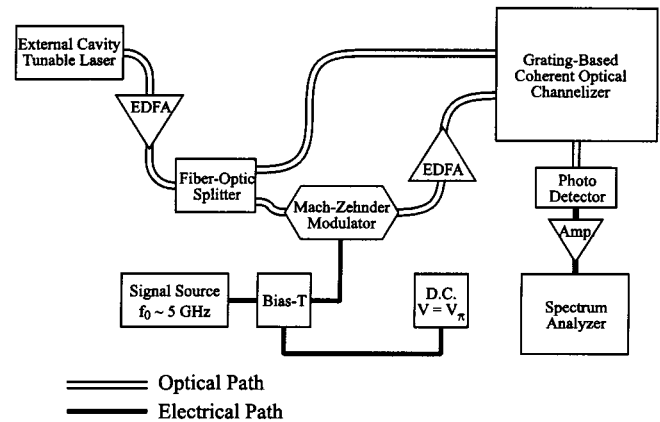


Fig. 4. Block diagram of the basic RF characterization setup.

Whereas the optimum split ratio is 75% transmission and 25% reflection, the measured transmission and reflection coefficients for the beamsplitter in our lens assembly were 84% and 6%, respectively, with a 10% loss apparently due to absorption in the beamsplitter's dielectric layer. This essentially accounts for the difference in the optical insertion losses for the two paths.

As mentioned above, our analysis showed that it is desirable to spread the signal beam spot by a factor of 3–4 with respect to the LO spot. In order not to increase the insertion loss unduly, the spreading should be only along the direction parallel to the grating-induced dispersion. We constructed an anamorphic imaging system that transformed the circular mode pattern emerging from the signal beam input fiber into an elliptical pattern whose minor axis is equal to the fiber's mode diameter, and whose major axis is expanded threefold. When the elliptical beam waist was positioned in the input plane of the channelizer's signal port, the optical insertion loss for the signal beam path increased to 31 dB.

#### IV. CHARACTERIZATION OF THE COHERENT OPTICAL RF CHANNELIZER

##### A. Experiment Setup

There are several important figures-of-merit for a photonic channelizer: i.e., insertion loss, channel response uniformity (ripple), crosstalk, and SFDR. The basic experimental setup used for these measurements is shown schematically in Fig. 4. An external cavity semiconductor laser (ECSL) at 1550 nm was amplified by an erbium-doped fiber amplifier (EDFA), and then split by a fiber-optic coupler to two paths. One of the beams was sent through a polarization controller then directly to the LO port of the optical channelizer and the other to a traveling wave  $\text{LiNbO}_3$  Mach-Zehnder modulator (MZM). The MZM had a push-pull electrode configuration and was operated at the low-intensity or null-bias point. The combination of push-pull electrodes and null-bias operating condition is necessary to insure complete suppression of the carrier and all even-order harmonics in the modulated optical field, while simultaneously maximizing the fundamental component of the signal. The output from the modulator was directed to a second EDFA followed by a polarization controller then into the signal-input port of the optical channelizer. The LO and signal beams were

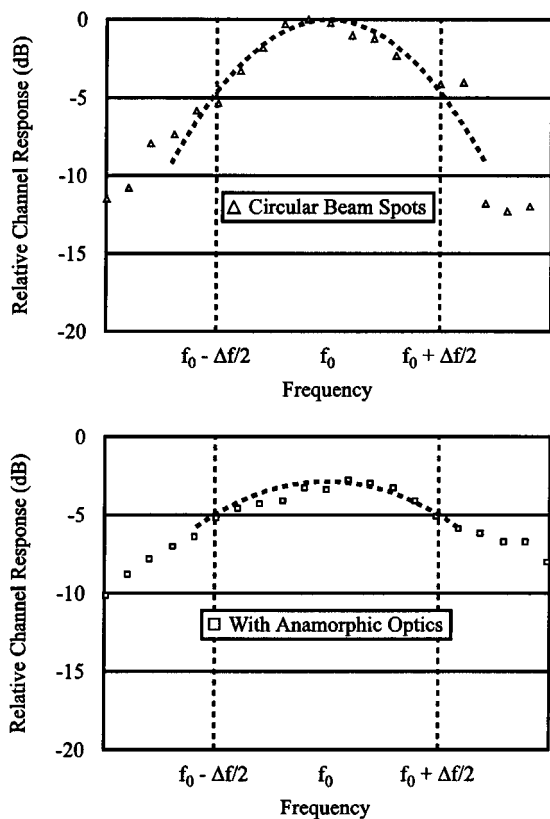


Fig. 5. Comparison of the channel response for the two optical configurations described in the text. Center frequency is  $f_0 = 5$  GHz. Channel width is  $\Delta f = 1$  GHz.

positioned in the input plane in such a fashion to produce a 5-GHz offset between the two at the output. After being collected in the multimode fiber as described above, the beams were fed to a high-speed photodetector. The detector's output was amplified and the electronic signal was displayed on a spectrum analyzer.

### B. Channel Frequency Response

To determine the channel frequency response, a CW tone was applied to the MZM. The focused spot produced at the output focal plane by one of the sidebands was overlapped with that of the LO. The heterodyne signal generated at the photodetector was maximized for an RF signal at about 5 GHz. We determined the channel response by measuring the power in the heterodyne beat note as we varied the RF frequency about the channel center frequency. We measured channel response with and without the anamorphic optics, and the results are shown in Fig. 5. In the figure, the signal levels are normalized to the response at the center of the channel for the circular beam spot case. The dashed lines in the figures are the calculated channel responses based on Gaussian spot profiles fitted to the data.

The inclusion of the anamorphic optics clearly improved channel response uniformity as expected, although at a cost of some signal loss introduced by the increase in the insertion loss for the elliptical beam case, as noted above.

### C. Crosstalk

Following the convention used in RF channelized receivers, crosstalk is defined as the ratio of the response to a signal at the

center of channel  $f_0$  to that of a signal at the near edge of the next-nearest neighbor channel  $f_0 \pm 3/2\Delta f$ . In order to achieve low crosstalk and limit the noise bandwidth, the output of each channel would be equipped with an electronic bandpass filter that cuts off any frequency components out of the IF bandwidth  $f_0 \pm 1/2\Delta f$ . In that case, crosstalk will be a result of the mixing signal between the LO beam at  $f_0 \pm 2\Delta f$  and the signal beam at  $f_0 \pm 3/2\Delta f$ . Calculations based on Gaussian beam distributions indicated that crosstalk performance of better than 70 dB was obtainable.

In our measurement, the heterodyne signal level was first measured at the center of the channel  $f_0$ , and then measured again when the input signal port was moved to the location equivalent to  $f_0 \pm 3/2\Delta f$  and LO input port to  $f_0 \pm 2\Delta f$ . The output slit was kept at the same location during the process. The crosstalk at  $f_0 - 3/2\Delta f$  was measured to be  $>52$  dB, which was below the measurement system noise level. However, crosstalk of 35 dB was measured at  $f_0 + 3/2\Delta f$ . Since the optical channelizer lens measurement did not show high side-lobes, the higher than expected crosstalk must have been caused by other optical components used in the system. Further study of the beams at the output focal plane showed that the focused spot from the signal beam had good quality, but that from the LO beam had some sidelobe structure in the horizontal or the dispersion directions. The vertical beam scan from both input ports had very good quality. The only difference in the optical path for both ports was a beam turning microprism for the LO optical path. We believe the optical beam from the fiber had an angular distribution that was larger than the numerical aperture of the turning prism, which caused the loss of the total internal reflection for part of the LO beam. When we extended our measurement to one more channel away, i.e., at  $f_0 \pm 5/2\Delta f$ , the crosstalk in either direction was below the measurement noise level ( $>52$  dB).

### D. SFDR

When a null-biased MZM is used to impress the electronic signal on an optical carrier, the largest distortion products are the third-order two-tone intermodulation products. These limit the upper end of the channelizer's dynamic range because they appear as spurious components of the two-tone spectrum in adjacent channels. The maximum allowable signal level is reached when the heterodyne product of a two-tone signal spur and the LO equals the noise floor. The dynamic range is defined as the ratio of the signal power in the maximum allowable signal to the signal power that produces a fundamental response equal to the noise floor. Under such operating conditions, the SFDR can be written as

$$\text{SFDR} = \left( \frac{4Rs^2 P_{\text{sig}} G_{\text{sig}} T_{\text{sig}} P_{\text{LO}} G_{\text{LO}} T_{\text{LO}}}{P_{\text{noise}}} \right)^{2/3} \quad (1)$$

where  $R$  is the load resistor of the detector,  $s$  is the detector responsivity,  $P_{\text{sig}}$  is the optical power incident on the modulator,  $P_{\text{LO}}$  is the optical power in the LO for a given channel,  $G$  is the optical amplifier gain,  $T$  is the optical throughput for the signal and LO beampaths as indicated, and  $P_{\text{noise}}$  is the output noise power level. The noise power at the receiver in general

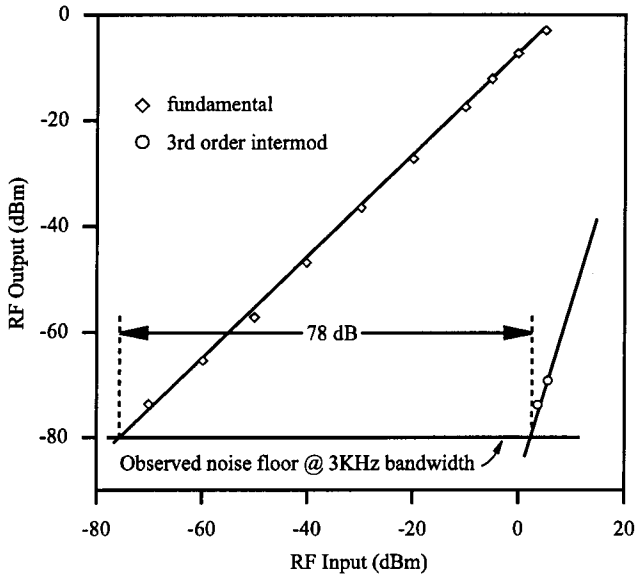


Fig. 6. Measurement of two-tone SFDR.

has contributions from thermal, shot, and amplified spontaneous emission (ASE) generated from the EDFAs. The noise power at the output can then be written as

$$P_{\text{noise}} = \left( 4kT + 2esP_{\text{LO}}G_{\text{LO}}T_{\text{LO}}R + 2h\nu s^2 F_{\text{sig}}G_{\text{sig}}T_{\text{sig}}P_{\text{LO}}G_{\text{LO}}T_{\text{LO}}R \right) B \quad (2)$$

where  $k$  is the Boltzman constant,  $T$  is the temperature,  $e$  is the electron charge,  $F_{\text{sig}}$  is the signal EDFA noise figure,  $h\nu$  is the photon energy, and  $B$  is the channel bandwidth.

A two-tone measurement was performed to determine the dynamic range of the photonic channelizer. First, the RF output level at a channel centered at 6 GHz was measured as a function of the input RF power level. We then applied equal amplitude tones at  $f_1 = 9$  and  $f_2 = 12$  GHz to the modulator through a 3-dB coupler. The  $2f_1 - f_2$  output tone at 6 GHz was measured as a function of the input RF power levels. The RF input power is the power in the signal (or each of the two signals in the IM3 measurement) applied to the modulator. The detector output was amplified by 49.6 dB and was then fed to a spectrum analyzer. The fundamental and third harmonic signal levels are plotted against the input RF signal level in Fig. 6.

We measured an SFDR of 78 dB into the 3-kHz noise bandwidth, which equates to  $101 \text{ dB} \cdot \text{Hz}^{2/3}$ . Based on the optical power levels from the LO and signal beam paths, and the EDFA gain and measured ASE power spectral density, we would expect to have an SFDR of about  $107 \text{ dB} \cdot \text{Hz}^{2/3}$ . Of this 6-dB difference, we were able to attribute 2 dB to excessive noise levels, and the other 4 dB is due to the observed link gain for our channelizer being lower than the calculated value.

## V. CONCLUSION AND DISCUSSION

In conclusion, we have demonstrated a prototype optical channelizer based on a free-space diffraction grating. Our

optical channelizer exhibited sufficient dispersion and beam quality for a 1-GHz channel spacing and a total instantaneous bandwidth of well over 100 GHz. We further demonstrated the feasibility of using heterodyne detection to perform the frequency translation to a common IF for all the channels. The RF receiver performance, including the channel frequency-response uniformity, crosstalk, and SFDR, has been characterized and compared to our theoretical prediction with good agreement. We also determined that the system's photonic link gain (the ratio of the RF power out of the detector to the RF power input to the modulator) was  $-90$  dB, and the photonic link noise figure was 60 dB. Both of these values are due to the high end-to-end optical losses experienced in our system. The link gain and noise figure, as well as the dynamic range, can be significantly improved by the reduction of the insertion loss. For example, elimination of the excess insertion loss in the free-space portion of the optical paths for the signal and LO beams would improve the link gain to about  $-40$  dB and the noise figure to 32 dB. This improvement can be achieved by introducing more custom-made optics and removing the beam-splitting prism. Additional performance gains will be realized as the photonic components, such as the lasers, modulators, and detectors are improved. For practical field deployment in typical environment, new designs based on rigid physical structures, other than off-the-shelf commercial optics, needs to be developed. Additionally, techniques exist for actively monitoring and controlling such things as optical path lengths and component alignment that could be employed in this system [13]. Further work on reducing the optical insertion loss and physical size will make the photonic channelizer's insertion into wide-band RF systems practical.

## ACKNOWLEDGMENT

The authors would like to thank N. Nelson, TRW, Redondo Beach, CA, for his help in the optical channelizer lens characterization.

## REFERENCES

- [1] J. P. Lindley and H. L. Nurse, "Spectrum analysis using acousto-optic techniques," *Proc. SPIE-Int. Soc. Opt. Eng.*, vol. 128, pp. 119-126, 1977.
- [2] A. Vanderlugt, "Interferometric spectrum analyzer," *Appl. Opt.*, vol. 20, p. 2770, 1981.
- [3] T. Bader, P. Kellman, and H. Shaver, "Time integrating optical processing," AFO Sci. Res., Final Tech. Rep. AFO Sci. Res. Contract F49260-78-C-0102, 1981.
- [4] I. C. Chang, "Wideband acousto-optic spectrometer," *Proc. SPIE-Int. Soc. Opt. Eng.*, vol. 1476, pp. 257-268, 1991.
- [5] E. M. Alexander and A. E. Spezio, "New method of coherent frequency channelization," *Proc. SPIE-Int. Soc. Opt. Eng.*, vol. 352, pp. 228-231, 1982.
- [6] E. M. Alexander and R. W. Gammon, "The Fabry-Perot etalon as an RF frequency channelizer," *Proc. SPIE-Int. Soc. Opt. Eng.*, vol. 464, pp. 45-52, 1984.
- [7] E. M. Alexander, "Optical techniques for wide bandwidth microwave spectrum analysis," *Proc. SPIE-Int. Soc. Opt. Eng.*, vol. 789, pp. 169-175, 1987.
- [8] J. M. Heaton, C. D. Watson, S. B. Jones, M. M. Bourke, C. M. Boyne, G. W. Smith, and D. R. Wright, "Sixteen channel (1 to 16 GHz) microwave spectrum analyzer device based on a phased-array of GaAs/Al-GaAs electro-optic waveguide delay lines," *Proc. SPIE-Int. Soc. Opt. Eng.*, vol. 3278, pp. 245-251, 1998.

- [9] T. Jung, J. L. Shen, D. T. K. Tong, S. Murthy, M. C. Wu, T. Tanbun-Ek, W. Wang, R. Lodenkamper, R. Davis, L. J. Lembo, and J. C. Brock, "CW injection locking of a mode-locked semiconductor laser as a local oscillator comb for channelizing broad-band RF signals," *IEEE Trans. Microwave Theory Tech.*, vol. 47, pp. 1225–1233, July 1999.
- [10] R. T. Logan, "All-optical heterodyne RF signal generation using a mode-locked-laser frequency comb: Theory and experiments," in *IEEE MTT-S Int. Microwave Symp. Dig.*, vol. 3, 2000, pp. 1741–1744.
- [11] R. Lodenkamper, T. Jung, R. L. Davis, L. J. Lembo, M. C. Wu, and J. C. Brock, "RF performance of optical injection locking," *Proc. SPIE-Int. Soc. Opt. Eng.*, vol. 3463, pp. 227–236, 1998.
- [12] R. Lodenkamper, R. L. Davis, L. J. Lembo, M. G. Wickham, and J. C. Brock, "Evaluation of optical channelizers in terms of RF performance," *Proc. SPIE-Int. Soc. Opt. Eng.*, vol. 3463, pp. 200–211, 1998.
- [13] M. C. Wickham and E. Upton, "Precise adaptive photonic RF filters realized with adaptive Bragg gratings," *Proc. SPIE-Int. Soc. Opt. Eng.*, vol. 4112, pp. 109–114, 2000.

**Wenshen Wang** (S'93–M'95) received the B.Eng. and M.Eng. degrees from Tsinghua University, Beijing, China, in 1983 and 1986, respectively, and the Ph.D. degree in electrical engineering from the University of California at Los Angeles, in 1995.

From 1995 to 1997, he was a Staff Scientist with the TACAN Corporation, where he was involved with novel photonic devices and applications. In 1997, he was a Senior Member Technical Staff with TRW Inc., Redondo Beach, CA, where he performed research on photonic devices and systems. In 2000, he joined New Focus Inc., Santa Clara, CA, where he develops novel photonic devices.

**Richard L. Davis** (M'87) received the B.S. degree in physics from the California State University, Long Beach, in 1972, and the M.S. degree in physics from the University of California at Los Angeles (UCLA), in 1973.

He is currently a Senior Staff Engineer at TRW Inc., Redondo Beach, CA, where he applies over 25 years of experience in a wide range of photonics technologies. His research activities include optical signal processing, integrated-optical sensors, fiber-optic communication systems, optical neural networks, and holographic memories.

**Thomas J. Jung** (S'97) received the B.S. and M.S. degrees in electrical engineering from the University of California at Los Angeles, in 1996 and 1998, respectively.

Since 1996, he has been a Member of the Technical Staff with the Photonics Technology Department, TRW Inc., Redondo Beach, CA. His research interests include ultrafast integrated optoelectronics, microwave photonics, and EO sampling of high-speed devices.

**Robert Lodenkamper** (M'01), photograph and biography not available at time of publication.

**Lawrence J. Lembo** (M'95), photograph and biography not available at time of publication.

**John C. Brock** (M'94) received the B.S. degree in chemistry from the University of Washington, Pullman, in 1972, and the Ph.D. degree in chemistry from the University of California at Berkeley, in 1976.

He held a post-doctoral position in environmental engineering at the California Institute of Technology, prior to joining the Atmospheric Chemistry Group, Jet Propulsion Laboratory. In 1980, he joined TRW Inc., where he was involved with chemical lasers, nonlinear optics, and high-performance optoelectronics for analog application. He is currently the Director of Photonic Engineering with Velocium, Redondo Beach, CA.



**Ming C. Wu** (S'82–M'83–SM'00) received the M.S. and Ph.D. degrees in electrical engineering from the University of California at Berkeley, in 1985 and 1988, respectively.

From 1988 to 1992, he was a Member of Technical Staff at AT&T Bell Laboratories, Murray Hill, NJ, where he conducted research in high-speed semiconductor lasers and optoelectronics. In 1993, he joined the faculty of the Electrical Engineering Department, University of California at Los Angeles (UCLA), where he is currently a Professor. He has authored or co-authored over 100 journal papers, 180 conference papers, contributed one book chapter, and holds eight U.S. patents. His current research interests include microelectromechanical systems (MEMS), microoptical electromechanical systems (MOEMS), ultrafast integrated optoelectronics, microwave photonics, high-power photodetectors, and modulators.

Dr. Wu is a member of the American Physical Society, the Optical Society of America, the International Scientific Radio Union (URSI), and Eta Kappa Nu. He is the director of the Multiuniversity Research Initiative (MURI) Center on RF Photonic Materials and Devices sponsored by the Office of Naval Research (ONR) and a member of the California NanoSystem Institute (CNSI). He was general co-chair of the IEEE Lasers and Electro-Optics Society (IEEE LEOS) Summer Topical Meeting in 1995 (RF Optoelectronics), 1996 and 1998 [Optical Microelectromechanical Systems (MEMS)], and 1998 International Conference on MOEMS. He has also served on the Program Committees of the Optical Fiber Communication Conference (OFC), Conference on Lasers and Electro Optics (CLEO), MEMS, Optical MEMS, International Electron Device Meeting (IEDM), and Device Research Conference (DRC). He was the recipient of the 1992 Packard Foundation Fellowship and the 1994 Meritorious Conference Paper Award of the Government Microcircuit Applications Conference (GOMAC).